DOI: 10.48011/asba.v2i1.1051

Power Control for a Wind Power Generation from SCIG and Harmonic Current Filtering

Ângelo Marcílio M. dos Santos [*]
Ricardo Parcelle C. Pacífico [**] **Leonardo P. S. Silva** [**]
Marcos Vinícius S. França [**]
Vanessa Siqueira de C. Teixeira [*] **Adson Bezerra Moreira** [*]

[*] *PPGEEC/UFC, Campus Sobral, Federal University of Ceará, Sobral-CE, Brazil, (e-mail: angelomarcilio@alu.ufc.br).*
[**] *Electrical Engineering, Campus Sobral, Federal University of Ceará, Sobral-CE, Brazil.*

Abstract: The main contribution of this paper is to present a proposal for the development of an active power filter (APF) for a wind power generation system connected to the electric grid, using the three-phase induction generator with squirrel cage rotor (SCIG). In the induction generator side converter (IGSC) the power control is done by the magnetizing current and electromagnetic torque in coordinates dq. Thus, the wind system controls the active and reactive powers, as well as performing the active filtering function in the grid currents. Harmonic compensation is performed by an algorithm applied to the grid side converter (GSC). That technique improves the power quality and keeps the voltage at DC bus. The studied system was mathematically modeled and simulated using the Matlab / Simulink software. When SCIG provides 2 kW of active power, the THD from 18,94% (without APF) was reduced to 3,93% for GSC operating with APF function.

Keywords: Electric power generation; Electronic back-to-back converter; SCIG; Wind energy; Active power filter; THD.

1. INTRODUCTION

With the progressive decline of fossil fuels reserves and ever-increasing demand of energy, the production of electric energy from renewable resources, such as solar, wind and tidal streams oceans, has now been accepted as a potentially promising solution to the energy problem. Wind power is an effective measure, and development of wind power generation has increasingly attracted attention in several countries (Chen et al., 2010).

There are several types of electric generators used in wind power system. Therefore, the choice of wich type of electric generator depends on the application of a distributed machine, wind farms, electric transmission, machine power and cost (Navas et al., 2015), (Mahajan et al., 2017).

The back-to-back converter is composed of two voltage source converters connected together via a DC bus capacitor. One converter stays between the SCIG and the DC bus capacitor, called induction generator side converter (IGSC), which has the function to produce the machine flux for SCIG and to optimum the energy capture from the wind. The second converter stays between the DC bus capacitor and the grid, called grid side converter (GSC), which has the function to regulate the DC bus voltage (HEYDARI et al., 2012).

The schematic diagram of the wind power generation system connected to the grid using SCIG is shown in the Fig. 1.

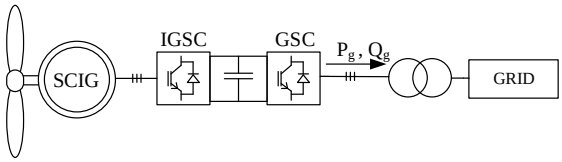

Figure 1. Traditional operation diagram of SCIG.

Power quality is an important factor in a power system connected to the electric grid. One of the main terms related to power quality they are the "harmonic", which are defined as alternating components with a frequency different from the fundamental frequency. Those harmonics are caused mainly by the use of electronic devices, resulting in the injection of harmonics into the grid, which distort the voltage and current waveforms of the grid. Harmonic components promote low power factor, voltage flickering (flicker), sudden voltage increases (swell), among others (Moreira et al., 2019).

Active filtration is a widespread solution to reduce harmonic currents. The active power filter (APF) detects the harmonic current of the nonlinear load and injects a current compensation to mitigate the harmonic components in the grid. The control strategy to mitigate the harmonic current components in the electric grid can be accomplished through modifications in the GSC control (Souza et al., 2018).

This work proposes a control strategy for a wind system using SCIG. In addition to power control, the system

improves power quality using the GSC to perform active filtering at the point of common coupling (PCC) at dq coordinates.

The Fig. 2 shows the control scheme for the SCIG / APF. The operation diagram ilustrates how occurs the power generation and the harmonic current mitigation for the system connected to electric grid. Simulation results obtained are presented to prove the idea of this paper.

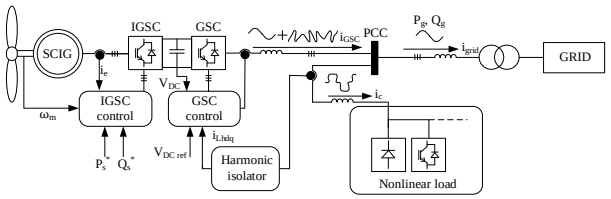

Figure 2. Operation diagram for the proposed SCIG/ APF.

2. POWER CONTROL OF THE SQUIRREL CAGE INDUCTION GENERATOR (SCIG)

In SCIG the rotor terminals are shorted and the rotor current is not measured. Then, $V_{rdq} = 0$ and i_{rdq} are not measured. Thus, the rotor currents in dq coordinates are given by (1) and (2), where V_{rdq} are the voltages in the rotor, i_{rdq} are the currents in the rotor, i_{edq} are the currents in the stator, $\hat{i}_{mr}$ is the magnitude of the magnetizing current, σ_r is the dispersion factor of the rotor, θ_r is the rotation angle of the rotor and ρ is the angle of the rotating axis of stator voltages and currents (Navas et al., 2015).

$$i_{rd} = \frac{\hat{i}_{mr} \; - \; i_{ed}}{1 + \sigma_r} \; e^{-j\theta_r} \tag{1}$$

$$i_{rq} = \frac{-\; i_{eq}}{1 + \sigma_r} \; e^{-j\theta_r} \tag{2}$$

The electromagnetic torque and the rotor time constant (τ_r) are defined in (3) and (4), where L_m is the magnetization inductance, and R_r is the rotor resistance.

$$T_e = \frac{3}{2} \; \frac{L_m}{1 \; + \; \sigma_r} \; \hat{i}_{mr} \; i_{eq} \tag{3}$$

$$\tau_r = \frac{L_m \; (1 \; + \; \sigma_r)}{R_r} \tag{4}$$

The rotating magnetic field speed and the rotor speed are determined in (5) and (6).

$$\omega_m = \frac{d\rho}{dt} \tag{5}$$

$$\omega_r = \frac{d\theta_r}{dt} \tag{6}$$

In SCIG the flux observer is required to obtain the magnetizing current, the rotating field angle and the speed of the rotating field.

The flux observer is performed by the block diagram of Fig. 3, and is based on (7) and (8), where $\hat{i}_{mr}$ is set to a constant value ($\hat{i}_{mr} = i_{ed}$), what is required for a linear torque control by i_{eq} (Yazdani and Iravani, 2010).

$$\tau_r \; \frac{d}{dt} \; [\hat{i}_{mr}] \; = -\hat{i}_{mr} \; + \; i_{ed} \tag{7}$$

$$\omega_m = \frac{i_{eq}}{\tau_r \; \hat{i}_{mr}} \; + \; \omega_r \tag{8}$$

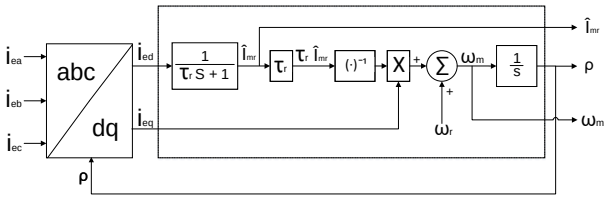

Figure 3. Flux observer block diagram.

The magnetizing current reference and electromagnetic torque reference are obtained by (9) and (10), where V_{en} is the rated line voltage of the stator, σ_e is the dispersion factors of the stator, ω_{m0} is the rated angular speed of the generator ($\omega_{m0} \; = \; 2 \; \pi \; f_{m0}$) and P_{ref} is the desired reference power.

$$\hat{i}_{mr-ref} = \sqrt{\frac{2}{3}} \; \frac{V_{en}}{(1 \; + \; \sigma_e) \; L_m \; \omega_{m0}} \tag{9}$$

$$T_{eref} = \frac{P_{ref}}{\omega_r} \tag{10}$$

The vector control of the SCIG as function of the rotor coordinates is shown in Fig. 4, where $G_{ig}(s)$ is a PI controller.

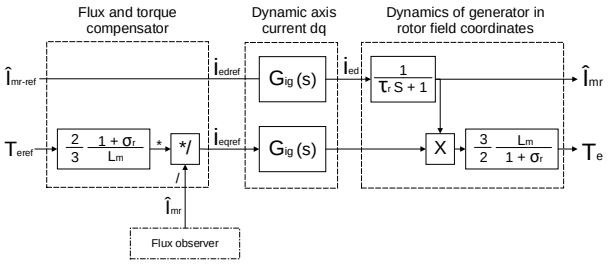

Figure 4. Block diagram of the vector control of the SCIG as a function of the coordinates of the rotor field.

Fig. 5 shows the block diagram of the IGSC control, where $G_{ig}(s)$ is a PI controller, R_e is the stator resistance and τ_e is the stator time constant. The IGSC controls the active and reactive powers of SCIG.

2.1 Grid Side Converter (GSC)

The grid side converter is an three-phase DC-to-AC electronic converter, what controls the DC bus voltage and injects current into the grid. The GSC control is performed by the block diagram of Fig. 6, what the current loop is shown in (a) and the voltage loop in (b) (Yazdani and Iravani, 2010).

The PLL (phase locked loop) is responsible for maintaining the synchronism between the voltages of the grid and those produced by the inverter, generating an angle θ in phase with the grid voltage, where V_A, V_B and V_C are grid line voltages (Moreira et al., 2019).

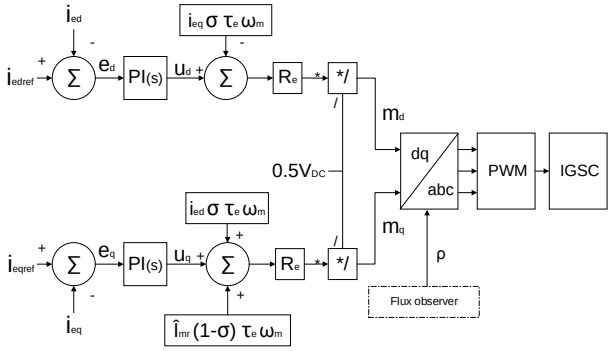

Figure 5. Current Control Loop of IGSC.

The signal reference generator (Fig. 6) produces the current references I_{dref} and I_{qref} from (11) and (12), where V_d and V_q are the dq voltages of the grid, i_d and i_q are the d-q currents of the grid, P_{ref} and Q_{ref} are references of active and reactive powers.

$$P_{ref} = \frac{3}{2}[V_d i_{dref} + V_q i_{qref}] \tag{11}$$

$$Q_{ref} = \frac{3}{2}[-V_d i_{qref} + V_q i_{dref}] \tag{12}$$

Since $V_q = 0$, (11) and (12) can be simplified as (13) and (14).

$$i_{dref} = \frac{2}{3V_d} P_{ref} \tag{13}$$

$$i_{qref} = -\frac{2}{3V_d} Q_{ref} \tag{14}$$

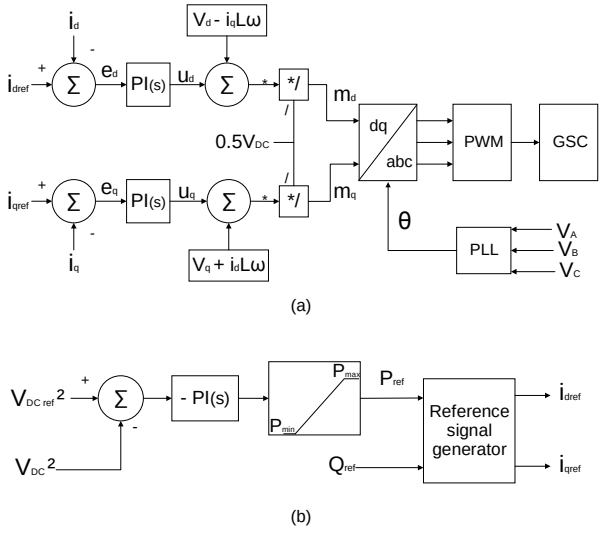

Figure 6. Control scheme of grid side converter (current loop (a) and voltage loop (b)).

3. ACTIVE POWER FILTER (APF)

The grid current can be distorted with a nonlinear load at the PCC. Thus, with the purpose to reduce the distortion of the grid current is used the APF.

The converter acting as an active filter must be capable of to inject a current that added to the load current, produce a "clean" current in the grid (Moreira et al., 2019).

For the inclusion of the APF function in the GSC, the structure of GSC control is modified, adding i_{Lhd} in the current control loop i_d and i_{Lhq} in the current control loop i_q. The modification keeps the voltage on the DC bus voltage and allows to mitigate harmonics current in the electric grid, as shown in the control diagram in Fig. 7.

For the proposed APF, the new references currents of the GSC for harmonic compensation are i^*_{dref} and i^*_{qref}, given in (15) and (16), where i_{Lhd} and i_{Lhq} are the harmonic components of the nonlinear load current.

$$i^*_{dref} = i_{dref} + i_{Lhd} \tag{15}$$

$$i^*_{qref} = i_{qref} + i_{Lhq} \tag{16}$$

The current of the electric grid is filtered in the PCC from the measurement of the currents of the three-phase nonlinear load and extracting the desired components. The components of measured currents are transformed to dq coordinates (i_{Ld}, i_{Lq}). The currents of the three-phase nonlinear load (i_{Lhd}, i_{Lhq}) are processed by low pass filters to extract the fundamental component, as shown in Fig. 8.

The fundamental component of the current is obtained from total load current. Therefore the harmonic components currents are isolated from (17) and (18), where i_{Lhd} and i_{Lhq} are the fundamental components of the current of nonlinear load.

$$i_{Lhd} = i_{Ld} - i_{Lfd} \tag{17}$$

$$i_{Lhq} = i_{Lq} - i_{Lfq} \tag{18}$$

To evaluate the harmonic current content, the total harmonic distortion (THD) is considered. THD calculation is given in (19), where I_1 is the fundamental component and I_h is the h-th harmonic current component of the electric grid. For the THD calculation interharmonic components are not considered.

$$THD(\%) = 100\frac{\sqrt{\sum_{h=2}^{50} I_h^2}}{I_1} \tag{19}$$

4. SIMULATION RESULTS AND DISCUSSION

The wind power generation system shown in Fig. 2 was implemented in the Matlab/Simulink software in order to analyze the proposed SCIG / APF control strategy. The

parameters of the generation system used in the simulation are shown in Table 1, where the SCIG parameters were obtained in (HEYDARI et al., 2012). The switching frequency of the converters is 10 kHz.

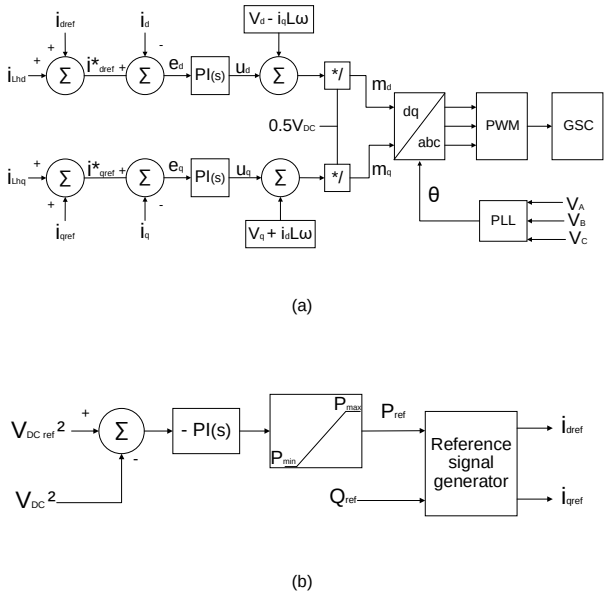

Figure 7. Control scheme of GSC with proposed active filter (current loop (a) and voltage loop (b)).

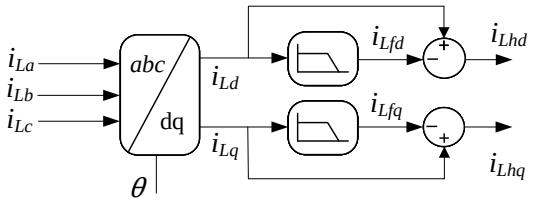

Figure 8. Harmonic current isolator.

Table 1. Simulation parameters.

	Parameters	Values
SCIG	P_n, V_n, F_n, P	$15kW$, $460V$, $60Hz$, 4
SCIG	R_e, R_r, $L_e = L_r$	$276.1m\Omega$, $164.5m\Omega$, $78.3mH$
SCIG	L_m, L_{le}, L_{lr}	$76.14mH$, $2.191mH$, $2.191mH$
GSC	L, R, C	$6mH$, $0,8\Omega$, $3500\mu F$
Load	R_L, L_L, L_{iL}	10Ω, $2mH$, $3,5mH$
Grid	V_{LL}, F	$380V$, $60Hz$

The simulation of the wind system was carried out with variable speed, and the generator operates with a speed of 150 rad/s and 200 rad/s.

4.1 Case 1 - Without APF

In the first case, the wind turbine with SCIG operates providing 2kW. The Figure 9 illustrates the measured magnetizing current of the generator and its reference, and measured torque of the generator and its reference. As can be seen, the magnetization current and the torque follow its references, which proves the suitable functioning of the control. The Figure 10 shows the responses of IGSC current control loops.

The Figure 11 show the GSC currents in direct and quadrature axis following their references.

The active power generated from SCIG for variable speed is controlled by direct current axis and reactive power is indirectly controlled by quadrature current axis. The Figure 12 show the active and reactive generated by the system.

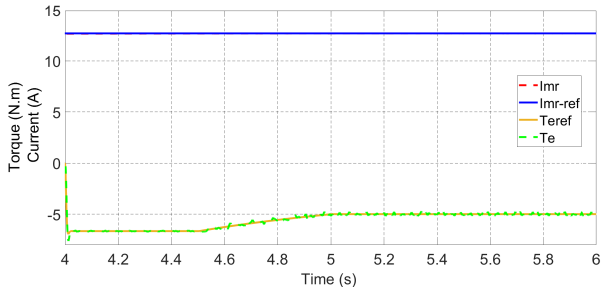

Figure 9. Torque and magnetizing current from generator.

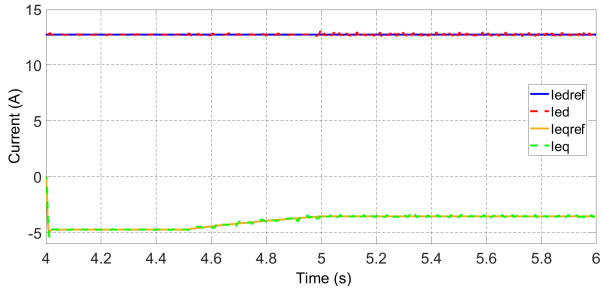

Figure 10. Response of control loop of the IGSC current controllers I_{ed} and I_{eq}.

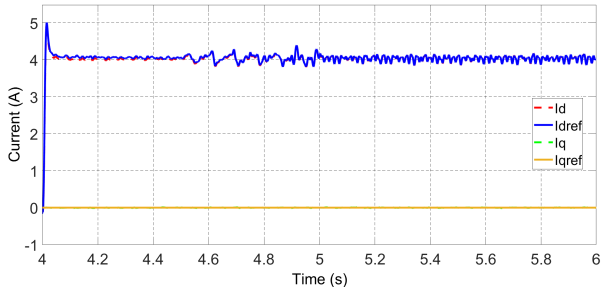

Figure 11. Response of control loop of the GSC current controllers I_d and I_q.

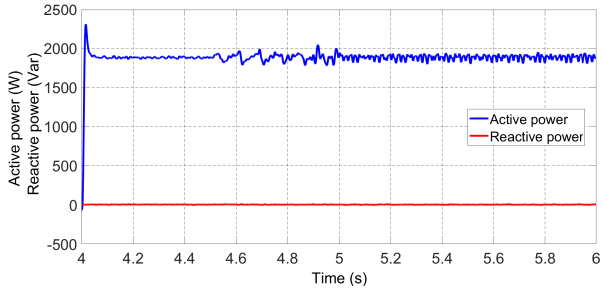

Figure 12. Response of active and reactive powers delivered at PCC.

The Fig. 13 shows the reference voltage of the DC bus and the voltage measured on the DC bus voltage. It is possible to check the DC bus voltage control remains stable with voltage regulated to 800V, even with the speed variation of the electric generator.

The Fig. 14 shows the waveforms of the grid voltage (V_a), currents of the electric grid, GSC and load of the system operating without APF, feeding a nonlinear load.

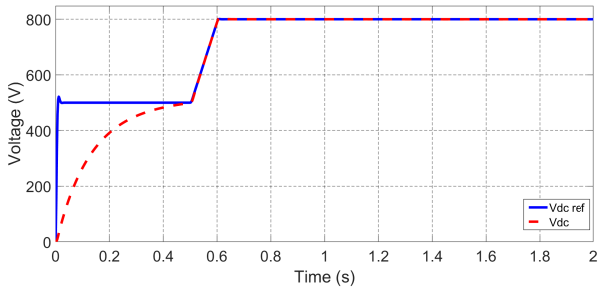

Figure 13. Response to DC bus voltage.

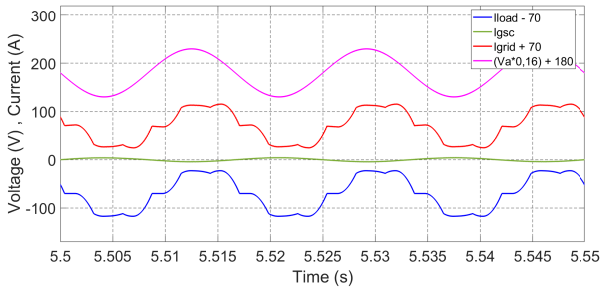

Figure 14. Waveforms of the voltage and current of the electric grid , currents of the load and from GSC when the system operates without APF.

The current spectrum of the nonlinear load is shown in Fig. 15. The waveform of load current is distorted and has a THD of 17,55%.

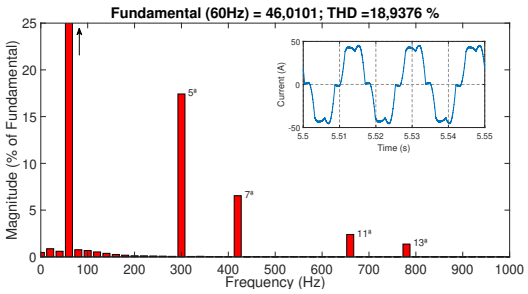

Figure 15. Spectrum of the nonlinear load current.

The Fig. 16 shows the current spectrum of the electric grid. The waveform of electric grid current is distorted and has a THD of 18.94%. This value is accordance with the main rules governing the connection of generators to the low voltage electrical grid, (IEEE, 2014) and (IEC, 2009).

The current spectrum of the electric grid shown by Fig. 16, it can be seen that the main harmonics that contributing to this distortion are those of an odd order (5 to and 7).

4.2 Case 2 - With APF

In the second case, the proposed APF was added to the system of wind power generation, being included in the GSC control.

The results related to the torque and magnetizing current from generator, control of the currents of the IGSC and the

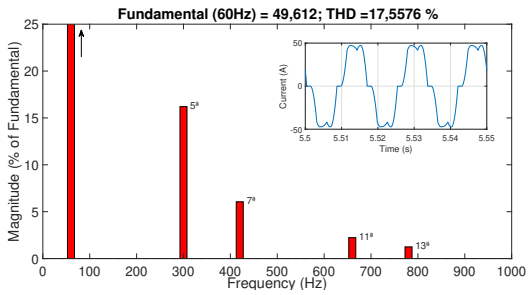

Figure 16. Spectrum of the grid current.

DC bus voltage presented behavior similar to the Figures 9, 10 and 13.

The Figures 17 and 18 show the currents in direct and quadrature axis of the GSC and the active and reactive power. It is possible to note that the GSC current references changes with the inclusion of harmonic filtering, which is due to the harmonic currents of the identified non-linear load being added to the current meshes of the AC / DC electronic converter. In addition, it is possible to note a slight change in reactive power, since with the addition of active filtration to the wind system, it starts to feed the non-linear load entirely.

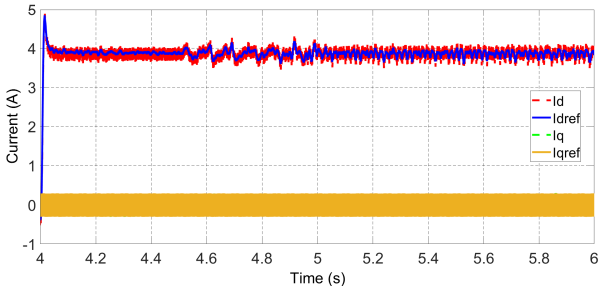

Figure 17. Response of control loop of the GSC current controllers I_d and I_q.

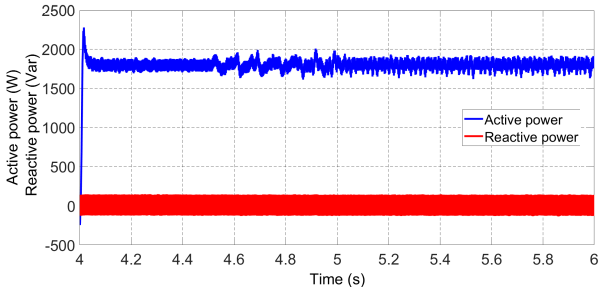

Figure 18. Response of active and reactive powers delivered at PCC.

Fig. 19 shows the waveforms of the electric grid voltage (V_a), currents of the electric grid, GSC and load system operating with APF, feeding a nonlinear load.

In Fig. 19, the current waveform of the electric grid is sinusoidal, different from the situation presented shown in Fig. 14, due to harmonic compensation current produced by the active power filter.

Fig. 20 shows The THD obtained for one phase of grid current was 3.92%. The THD value obtained is adequate in

accordance with the main rules governing the connection of generators to the low voltage electrical grid.

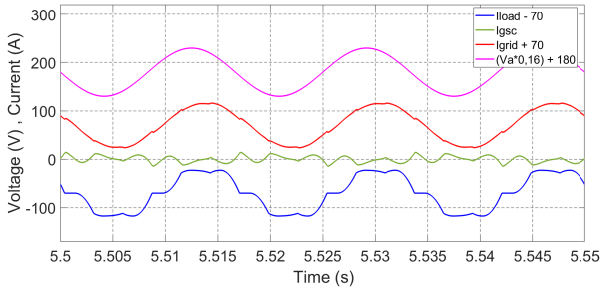

Figure 19. Waveforms of the voltage and current of the electric grid , currents of the load and from GSC when the system operates with APF.

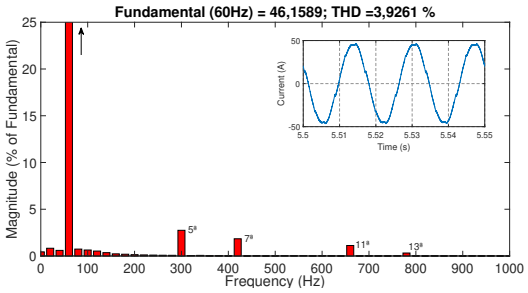

Figure 20. Spectrum of the grid current with APF.

When analyzing spectrum of electric grid with power system operating in tradicional mode (case 1) and with APF incorporated to the system (case 2), it is possible to observe an improvement in the THD of the electric current was reduced from 18.94% to 3.92%, and that the odd harmonic components are attenuated.

5. CONCLUSION

This work investigates the behavior of a wind power system with SCIG operating in a traditional mode (case 1) and operating with an active power filter (case 2). In both cases, the active and reactive powers delivered to the grid and the DC bus voltage remain at the same values, which proves that the system control behavior for both cases is satisfactory.

When analyzing the harmonic spectrum of the electric current before the harmonic compensation and after the harmonic compensation, THD was reduced from 18.94% to 3.86%, proving the good functioning of the APF and attesting that the harmonic compensation strategy incorporated into the wind power generation system with SCIG improves power quality, as shown by the simulation results.

REFERENCES

Chen, Y., Yang, Y., Wang, L., Jia, Z., and Wu, W. (2010). Grid-connected and control of mppt for wind power generation systems based on the scig. *2nd Int. Asia Conf. Informatics Control. Autom. Robot*, 03, 51–54.

HEYDARI, M., VARJANI, A.Y., and MOHAMADIAN, M. (2012). A novel variable-speed wind energy system using induction generator and six-switch ac/ac converter. *3rd Power Electronics and Drive Systems Technology (PEDSTC)*.

IEC, I.E.C. (2009). Iec 61000-3-2: Electromagnetic compatibility (emc) - part 3: Limits - section 2: Limits for harmonic current emissions (equipment input current < 16a per phase). *International Electrotechnical Commission (IEC)*, 05.

IEEE (2014). Ieee recommended practices and requirements for harmonic control in electric power system. *Project IEEE-519*.

Mahajan, S., Subramaniam, S.K., Natarajan, K., Gounder, A.G.N., and Borru, D.V. (2017). Analysis and control of induction generator supplying standalone ac loads employing a matrix converter. *Eng. Sci. Technol. an Int. J., vol. 20, no. 2, pp. 649–661, 2017, doi: 10.1016/j.jestch.2017.02.006.*

Moreira, A.B., Barros, T.A.D.S., Teixeira, V.S.D.C., Souza, R.R.D., Paula, M.V.D., and Filho, E.R. (2019). Control of powers for wind power generation and grid current harmonics filtering from doubly fed induction generator: Comparison of two strategies. *IEEE Access, vol. 7, no. c, pp. 32703–32713, 2019, doi: 10.1109/ACCESS.2019.2899456.*

Navas, M.A.H., Puma, J.L.A., and Filho, A.J.S. (2015). Direct torque control for squirrel cage induction generator based on wind energy conversion system with battery energy storage system. *IEEE Work. Power Electron. Power Qual. Appl. PEPQA*.

Souza, R.R., Moreira, A.B., Barros, T.A.S., and Filho, E.R. (2018). A proposal for a wind system equipped with a doubly fed induction generator using the conservative power theory for active filtering of harmonics currents. *Electr. Power Syst. Res., vol. 164, no. August 2017, pp. 167–177, 2018, doi: 10.1016/j.epsr.2018.07.027.*

Yazdani, A. and Iravani, R. (eds.) (2010). *Voltage-sourced converters in power systems: modeling, control, and applications*. [S.l.]: John Wiley Sons.